

B_c meson rare decays in the light-cone quark model

Teng Wang¹, Tianbo Liu¹, Da-Xin Zhang¹, and Bo-Qiang Ma^{1,2, a}

¹ School of Physics and State Key Laboratory of Nuclear Physics and Technology, Peking University, Beijing 100871, China

² Center for High Energy Physics, Peking University, Beijing 100871, China

Received: date / Revised version: date

Abstract. We investigate the rare decays $B_c \rightarrow D_s(1968)\ell\bar{\ell}$ and $B_c \rightarrow D_s^*(2317)\ell\bar{\ell}$ in the framework of the light-cone quark model (LCQM). The transition form factors are calculated in the space-like region and then analytically continued to the time-like region via exponential parametrization. The branching ratios and longitudinal lepton polarization asymmetries (LPAs) for the two decays are given and compared with each other. The results are helpful to investigating the structure of B_c meson and to testing the unitarity of CKM quark mixing matrix. All these results can be tested in the future experiments at the LHC.

PACS. XX.XX.XX No PACS code given

1 Introduction

The investigation on heavy-quark mesons is an active frontier of particle physics. The study of heavy-quark meson decays not only gives us insights on the hadron structure such as the hadron wave function [1] and the hadron transverse momentum distribution [2,3], but also provides us an ideal field to study the mixing between different generations of quarks by extracting the Cabibbo-Kobayashi-Maskawa (CKM) matrix elements. The investigation of the CKM matrix elements in heavy-quark meson decay processes can help us to test the charge-parity (CP) violation in the standard model (SM) [4,5,6,7,8] and to search for new physics beyond the SM [9,10]. Among all the heavy-quark mesons, the B_c meson is of special interest because of its some unique properties. It is the lowest bound state composed of two heavy quarks (b and c) with explicit flavor numbers. Distinguished from other heavy quark bound states like charmonia ($c\bar{c}$ bound state) and bottomonia ($b\bar{b}$ bound state) with implicit flavor numbers, B_c can only decay via weak interaction. Thus, B_c meson provides us a chance to study the weak interaction and the CKM matrix elements with all three generations included. Compared with the study of the B meson, the B_c meson received less attention, because the production of B_c mesons requires a much higher energy which is inaccessible to most available colliders. However, it was predicted that B_c mesons can be generated dramatically via different ways [11,12,13,14,15,16,17] in experiments at the Large Hadron Collider (LHC) which is running now. Therefore, it is mature for us to study the B_c meson on many of its physical quantities experimentally.

Among all the B_c meson decay modes, the rare decays $B_c \rightarrow D_s(1968,2317)\ell\bar{\ell}$ induced by the flavor changing neutral currents (FCNCs) are the most exciting ones. FCNCs processes have received lots of attention since the CLEO's measurement of the radiative decay $b \rightarrow s\gamma$ [18]. The process $b \rightarrow s\ell\bar{\ell}$ which can only happen at loop level provides a sensitive and stringent test of the unitarity of the CKM mixing matrix. Thus, it can serve as a test for the validity of the SM.

The decay process $B_c \rightarrow D_s(1968)\ell\bar{\ell}$ has been studied in a number of models, such as quantum chromodynamics (QCD) sum rules (SR) and relativistic quark model (RQM) [19,20,21,22]. However, there are few investigations on the decay $B_c \rightarrow D_s^*(2317)\ell\bar{\ell}$ [23]. The $D_s^*(2317)$ meson is considered to be of controversial since it was discovered in BaBar [24]. It was predicted to be broad and available to decay into DK and D^*K in the potential-based quark models [25,26]. However, the BaBar results show that $D_s^*(2317)$ is below the DK and D^*K thresholds and has a narrow decay width. Many works were done to clarify this disparity between theories and experiments. Some physicists advocated that $D_s^*(2317)$ is a DK molecular [27], a $D_s\pi$ atom [28] or a four-quark bound state [29], but some studies based on the heavy quark effective theory (HQET) [30,31] suggested that it is a conventional $c\bar{s}$ state. Following Ref. [30,31], we suppose that $D_s^*(2317)$ is a $c\bar{s}$ scalar meson with even parity. The study of form factors for $B_c \rightarrow D_s^*(2317)\ell\bar{\ell}$ process can also help us to learn more about the structure of $D_s^*(2317)$.

We choose the light-cone quark model (LCQM) [32,33,34] to perform the calculation in our work. LCQM takes an advantage of the equal light-cone time ($\tau = t+z/c$) quantization and includes the important relativistic effects which

^a e-mail: mabq@pku.edu.cn

are neglected in the traditional constituent quark model. In addition, compared with the complex vacuum in equal-time QCD, the vacuum in light-cone coordinates is simple, because the Fock vacuum state is the exact eigenstate of the full hamiltonian and all constituents in a physical eigenstate are directly related to that state. LCQM was widely used in the investigation of hadronic decays [35, 36, 37, 38] and electromagnetic transition form factors [39, 40], and it was proved successful in explaining the experimental data. We calculate the form factors, branching ratios and longitudinal lepton polarization asymmetries (LPAs) for the two decay processes in the framework of LCQM and compare the results with each other.

This paper is organized as follows. In Sect. 2, we discuss the standard model effective hamiltonian for $b \rightarrow s\ell\bar{\ell}$ decay. In Sect. 3, we calculate the hadronic form factors for the two decay processes in the light-cone framework. In Sect. 4 we present our numerical results. In Sect. 5, we give the discussion and conclusion.

2 Effective hamiltonian and form factors

The rare decay $B_c \rightarrow D_s\ell\bar{\ell}$ is described by $b \rightarrow s\ell\bar{\ell}$ transition at quark level. After integrating out heavy top quark and W^\pm bosons, one can write the effective interacting hamiltonian density responsible for this transition as [41]:

$$\begin{aligned} \mathcal{H}(b \rightarrow s\ell^+\ell^-) &= \frac{G_F\alpha}{\sqrt{2}\pi} V_{tb}V_{ts}^* [C_9^{\text{eff}}(m_b)\bar{s}_L\gamma_\mu b_L\bar{\ell}\gamma^\mu\ell \\ &\quad - \frac{2m_b C_7(m_b)}{q^2}\bar{s}_L i\sigma_{\mu\nu} q^\nu b_R\bar{\ell}\gamma^\mu\ell \\ &\quad + C_{10}(m_b)\bar{s}_L\gamma_\mu b_L\bar{\ell}\gamma^\mu\gamma_5\ell], \\ \mathcal{H}(b \rightarrow s\nu\bar{\nu}) &= \frac{G_F}{\sqrt{2}} \frac{2\alpha V_{tb}V_{ts}^*}{\pi\sin^2\theta_W} X(x_t)\bar{b}\gamma_\mu P_L s\bar{\nu}_l\gamma^\mu P_L \nu_l, \end{aligned} \quad (1)$$

where G_F is the Fermi constant, α is the electromagnetic fine structure constant and V_{ij} are the CKM matrix elements. $X(x_t)$, the top quark loop function, is given by:

$$X(x_t) = \frac{x_t(2+x_t)}{8(x_t-1)} + \frac{(3x_t-6)}{(1-x_t)^2} \ln x_t, \quad (x_t = \frac{M_t^2}{M_W^2})$$

and $C_i(\tilde{\mu})$ are the Wilson coefficients. In particular, C_9^{eff} , defined as an effective coefficient and containing the contribution from the charm-loop, is given by [42]:

$$\begin{aligned} C_9^{\text{eff}}(\tilde{\mu}) &= C_9 + (3C_1 + C_2 + 3C_3 + C_4 + 3C_5 \\ &\quad + C_6)h(\hat{m}_c, \hat{s}) - \frac{1}{2}h(0, \hat{s})(C_3 + 3C_4) \\ &\quad - \frac{1}{2}h(1, \hat{s})(4C_3 + 4C_4 + 3C_5 + C_6) \\ &\quad + \frac{2}{9}(3C_3 + C_4 + 3C_5 + C_6), \end{aligned} \quad (2)$$

where

$$\begin{aligned} h(\hat{m}_q, \hat{s}) &= -\frac{8}{9}\ln\frac{m_b}{\tilde{\mu}} - \frac{8}{9}\ln\hat{m}_q + \frac{8}{27} + \frac{4}{9}x - \frac{2}{9}(2+x) \\ &\quad \times |1-x|^{1/2} [\Theta(1-x)(\ln|\frac{\sqrt{1-x}+1}{\sqrt{1-x}-1}| - i\pi) \\ &\quad + \Theta(x-1)2\arctan\frac{1}{\sqrt{x-1}}], \end{aligned} \quad (3)$$

$$h(0, \hat{s}) = -\frac{8}{9}\ln\frac{m_b}{\tilde{\mu}} + \frac{8}{27} - \frac{4}{9}\ln\hat{s} + \frac{4}{9}i\pi, \quad (4)$$

in which $\hat{s} = q^2/m_b^2$, $\hat{m}_q = m_q/m_b$ and $x = 4m_q^2/q^2$, where m_q is the constituent quark mass.

In Eq. (3), we neglect long distance contributions from charmonia vector resonances $J/\Psi, \Psi', \dots$ [37, 43, 44]. To evaluate the decay rates and other physical quantities with this effective hamiltonian, we write the matrix elements of the effective nontrivial vertexes in Eq. (1) in terms of hadronic form factors:

$$\langle D_s(1968) | \bar{s}\gamma_\mu b | B_c \rangle = [f_+(q^2)P_\mu + f_-(q^2)q_\mu], \quad (5)$$

$$\begin{aligned} \langle D_s(1968) | i\bar{s}\sigma_{\nu\mu}\gamma_5 b q^\nu | B_c \rangle &= \frac{1}{M_{B_c} + M_{D_s}} \\ &\quad \times [q^2 P_\mu - (P \cdot q)q_\mu] F_T(q^2), \end{aligned} \quad (6)$$

$$\langle D_s^*(2317) | i\bar{s}\gamma_\mu\gamma_5 b | B_c \rangle = -[u_+(q^2)P_\mu + u_-(q^2)q_\mu], \quad (7)$$

$$\begin{aligned} \langle D_s^*(2317) | i\bar{s}\sigma_{\nu\mu}\gamma_5 b q^\nu | B_c \rangle &= \frac{1}{M_{B_c} + M_{D_s^*}} \\ &\quad \times [q^2 P_\mu - (P \cdot q)q_\mu] U_T(q^2), \end{aligned} \quad (8)$$

where $P = P_{B_c} + P_{D_s}$ and $q = P_{B_c} - P_{D_s}$. These form factors defined above are related to the commonly used Bauer-Stech-Wirbel (BSW) form factors [45] via:

$$\begin{aligned} F_1^{PP}(q^2) &= f_+(q^2), \\ F_0^{PP}(q^2) &= f_+(q^2) + \frac{q^2}{M_{B_c}^2 - M_{D_s}^2} f_-(q^2), \\ F_1^{PS}(q^2) &= u_+(q^2), \\ F_0^{PS}(q^2) &= u_+(q^2) + \frac{q^2}{M_{B_c}^2 - M_{D_s}^2} u_-(q^2). \end{aligned} \quad (9)$$

Then the differential decay rate of the exclusive processes $B_c \rightarrow D_s(1968)\ell\bar{\ell}$ can be expressed in terms of the form factors as:

$$\begin{aligned} \frac{d\Gamma(B_c \rightarrow D_s\ell^+\ell^-)}{d\hat{s}} &= \frac{G_F^2 M_B^5 \alpha^2}{3 \cdot 2^9 \pi^5} |V_{ts}^* V_{tb}|^2 \hat{\phi}^{\frac{1}{2}} (1 - 4\frac{m_\ell^2}{q^2})^{\frac{1}{2}} \\ &\quad \times \left[\hat{\phi} \left(1 + \frac{2m_\ell^2}{q^2} \right) f_{T+} + 6\frac{m_\ell^2}{q^2} f_{0+} \right], \\ \frac{d\Gamma(B_c \rightarrow D_s\nu\bar{\nu})}{d\hat{s}} &= \frac{G_F^2 M_B^5 \alpha^2}{2^8 \pi^5 \sin^4\theta_W} |X(x_t)|^2 |V_{ts}^* V_{tb}|^2 \hat{\phi}^{\frac{3}{2}} |f_+|^2, \end{aligned} \quad (11)$$

where

$$\begin{aligned} f_{T+} &= \left| C_9^{\text{eff}} f_+ - \frac{2C_7 F_T}{1 + \sqrt{\hat{r}}} \right|^2 + |C_{10} f_+|^2, \\ f_{0+} &= |C_{10}|^2 [(1 - \hat{r})^2 |f_0|^2 - \hat{\phi} |f_+|^2], \\ \hat{\phi} &= (\hat{s} - \hat{r} - 1)^2 - 4\hat{r}, \\ f_0 &= f_+ + \frac{q^2}{M_{B_c}^2 - M_{D_s}^2} f_-, \\ \hat{s} &= q^2/M_{B_c}^2, \quad \hat{r} = M_{D_s}^2/M_{B_c}^2. \end{aligned} \quad (12)$$

The longitudinal LPAs can be defined as:

$$P_L(\hat{s}) = \frac{d\Gamma_{h=-1}/d\hat{s} - d\Gamma_{h=1}/d\hat{s}}{d\Gamma_{h=-1}/d\hat{s} + d\Gamma_{h=1}/d\hat{s}}, \quad (13)$$

where the subscript h is the helicity of the ℓ^- in final states. From Eq.(13), we can obtain that [46]:

$$P_L(\hat{s}) = \frac{2(1 - 4\frac{m_l^2}{q^2})^{1/2} \hat{\phi} C_{10} f_+ \left[f_+ \text{Re} C_9^{\text{eff}} - \frac{2C_7 F_T}{1 + \sqrt{\hat{r}}} \right]}{\left[\hat{\phi} \left(1 + \frac{2m_l^2}{q^2} \right) F_{T+} + 6\frac{m_l^2}{q^2} f_{0+} \right]}. \quad (14)$$

For the case of $B_c \rightarrow D_s^*(2317)\ell\bar{\ell}$ processes, we just need to replace the form factors f_+ , f_- and F_T in Eq. (11) and Eq. (14) with u_+ , u_- and U_T respectively.

3 Form factors in light-cone framework

In LCQM, a meson can be considered as a quark-antiquark composed system. Assuming a meson with light-cone momentum $(P^+, (M^2 + P_\perp^2)/P^+, \mathbf{P}_\perp)$ is composed of two constituents q_1 and q_2 , we can give the light-cone components of the momenta p_1 and p_2 as:

$$\begin{aligned} p_1^+ &= xP^+, \quad p_2^+ = (1-x)P^+, \\ \mathbf{p}_{1\perp} &= x\mathbf{P}_\perp + \mathbf{k}_\perp, \quad \mathbf{p}_{2\perp} = (1-x)\mathbf{P}_\perp - \mathbf{k}_\perp. \end{aligned} \quad (15)$$

The light-cone wave function in the momentum space for a $^{2S+1}L_J$ meson is given by:

$$\begin{aligned} \Psi_{LS}^{JJ_z} &= \frac{1}{\sqrt{N_c}} \langle LS; L_z, S_z | LS; J, J_z \rangle \\ &\times R_{\lambda_1 \lambda_2}^{SS_z}(x, \mathbf{p}_\perp) \varphi_{LL_z}(x, \mathbf{p}_\perp), \end{aligned} \quad (16)$$

where $\langle LS; L_z, S_z | LS; J, J_z \rangle$ are the Clebsch-Gordon coefficients and $R_{\lambda_1 \lambda_2}^{SS_z}(x, \mathbf{p}_\perp)$ are the Melosh transformation [47, 48, 49, 50, 51, 52] matrix elements, which account for the relativistic effect due to quark transversal motions inside hadrons. Such an effect plays an important role to understand the famous proton “spin puzzle” [53, 54].

We use Gaussian-type wave functions [33] to describe the radial part $\varphi_{LL_z}(x, \mathbf{p}_\perp)$:

$$\varphi(x, \mathbf{p}_\perp)_{L=0} = \frac{4\pi^{3/4}}{\beta^{3/2}} \sqrt{\frac{dp_z}{dx}} \exp(-\frac{\mathbf{p}_\perp^2 + p_z^2}{2\beta^2}), \quad (17)$$

$$\varphi(x, \mathbf{p}_\perp)_{L=1} = \frac{4\sqrt{2}\pi^{3/4}}{\beta^{5/2}} \sqrt{\frac{dp_z}{dx}} p_{L_z} \exp(-\frac{\mathbf{p}_\perp^2 + p_z^2}{2\beta^2}), \quad (18)$$

where

$$p_{L_z=\pm 1} = \frac{\mp(p_x \pm ip_y)}{\sqrt{2}}, \quad p_{L_z=0} = p_z. \quad (19)$$

In the light-cone framework, p_z can be represented as:

$$p_z = (x - \frac{1}{2})M_0 + \frac{m_2^2 - m_1^2}{2M_0}, \quad (20)$$

where $M_0^2 = \sum_{i=1}^2 (\mathbf{k}_{\perp i}^2 + m_i^2)/x_i$ and m_i is the constituent quark mass.

For pseudoscalar mesons ($^{2S+1}L_J = ^1S_0$), the spin-orbit part $R_{\lambda_1 \lambda_2}^{SS_z}(x, \mathbf{p}_\perp)$ can be simplified as an effective vertex form:

$$R_{\lambda_1 \lambda_2}^{00}(x, \mathbf{p}_\perp) = -\frac{\bar{u}(p_1, \lambda_1) \gamma_5 v(p_2, \lambda_2)}{\sqrt{2}\widetilde{M}_0}, \quad (21)$$

where $\widetilde{M}_0 = \sqrt{M_0^2 - (m_1 - m_2)^2}$.

Correspondingly, for scalar mesons ($^{2S+1}L_J = ^3P_0$), we can also write an effective vertex by combining Clebsch-Gordon coefficients, spin-orbit part $R_{\lambda_1 \lambda_2}^{SS_z}(x, \mathbf{p}_\perp)$ and p_{L_z} in the radial part $\varphi(x, \mathbf{p}_\perp)_{L=1}$ together as [36]:

$$\begin{aligned} \langle 1S; L_z, S_z | 1S; J, J_z \rangle R_{\lambda_1 \lambda_2}^{1S_z}(x, \mathbf{p}_\perp) p_{L_z} \\ = i\bar{u}(p_1, \lambda_1) v(p_2, \lambda_2) \frac{\widetilde{M}_0}{\sqrt{6}M_0}. \end{aligned} \quad (22)$$

In LCQM, the Drell-Yan-West (DYW) ($q^+ = 0$) frame [55, 56] is widely used to calculate form factors. We can avoid the non-valence diagrams arising from the quark-antiquark pair creation (so-called Z-graph) [57] by choosing DYW frame. In this frame, the momenta of mesons in the initial and final states are represented as:

$$\begin{aligned} q &= (0, \frac{\mathbf{q}^2}{P^+}, \mathbf{q}_\perp), \quad P_{B_c} = (P^+, \frac{M_{B_c}^2}{P^+}, \mathbf{0}), \\ P_D &= (P^+, \frac{M_D^2 + \mathbf{q}_\perp^2}{P^+}, -\mathbf{q}_\perp), \end{aligned} \quad (23)$$

and the momenta of constituent quarks are represented as:

$$\begin{aligned} p_{\bar{c}} &= \left(xP^+, \frac{m_{\bar{c}}^2 + \mathbf{k}_\perp^2}{xP^+}, -\mathbf{k}_\perp \right), \\ p_b &= \left((1-x)P^+, \frac{m_b^2 + \mathbf{k}_\perp^2}{(1-x)P^+}, \mathbf{k}_\perp \right), \\ p_s &= \left((1-x)P^+, \frac{m_s^2 + (\mathbf{k}_\perp - \mathbf{q}_\perp)^2}{(1-x)P^+}, \mathbf{k}_\perp - \mathbf{q}_\perp \right). \end{aligned} \quad (24)$$

With the effective vertex and the wave functions given in Eq. (16)~Eq. (18), we can give the explicit forms of the

Table 1. The electro-weak parameters

Parameter	Value	Parameter	Value
m_W	80.41 GeV	C_1	-0.248
m_Z	91.837 GeV	C_2	1.107
$\sin^2 \theta_W$	0.2233	C_3	0.011
α^{-1}	129	C_4	-0.026
$ V_{tb}^* V_{ts} $	0.0385	C_5	0.007
C_6	-0.031	C_7	-0.313
C_9^{eff}	4.344	C_{10}	-4.669

form factors $f_+(q^2)$, $f_-(q^2)$, $F_T(q^2)$, $u_+(q^2)$, $u_-(q^2)$ and $U_T(q^2)$ (see in appendix).

Noticing that all the form factors are calculated in the space-like region with $q^2 = q^+ q^- - \mathbf{q}_\perp^2 \leq 0$, while B_c meson rare decays are defined in the time-like region, we need to parameterize the form factors as explicit functions of q^2 in the space-like region and then extended them through the analytical continuation to the time-like region. We choose a three-parameter form in this paper as:

$$F(q^2) = F(0) \exp[a(q^2/M_{B_c}^2) + b(q^2/M_{B_c}^2)^2], \quad (25)$$

where $F(q^2)$ denotes any one of the form factors used in this paper.

4 Numerical results

In this section, we calculate the form factors, branching ratios and longitudinal LPAs with input parameters. The Wilson coefficients and other electro-weak constants used in Eq. (1) and Eq. (11) are given in Table 1 [22]:

The constituent quark masses used in LCQM calculation are chosen as [58]:

$$m_s = 0.37 \text{ GeV}, \quad m_c = 1.4 \text{ GeV}, \quad m_b = 4.8 \text{ GeV}.$$

There is still another important parameter β which describes the momenta distribution of constituent quarks in Eq. (17) and Eq. (18). It can be fixed by meson decay constants as:

$$\begin{aligned} f_P &= 2\sqrt{6} \int \frac{dx d^2 \mathbf{k}_\perp}{16\pi^3} \frac{\mathcal{A}}{\mathcal{A}^2 + k_\perp^2} \varphi_s(x, \mathbf{k}_\perp), \\ f_S &= 2\sqrt{6} \int \frac{dx d^2 \mathbf{k}_\perp}{16\pi^3} \frac{m_1(1-x) - m_2 x}{\mathcal{A}^2 + k_\perp^2} \varphi_p(x, \mathbf{k}_\perp), \end{aligned} \quad (26)$$

where $\mathcal{A} = m_s(1-x) + m_b x$, f_P and f_S are the decay constants of pseudoscalar and scalar mesons, and φ_s and φ_p are s -wave and p -wave functions.

The decay constants of B_c , $D_s(1968)$ and $D_s^*(2317)$ mesons in this paper are employed as $f_{B_c} = 400 \pm 40 \text{ MeV}$ [59], $f_{D_s} = 257.8 \pm 5.9 \text{ MeV}$ [60] and $f_{D_s^*} = 71 \text{ MeV}$ [61]. Then, we can fix the β parameters as: $\beta_{B_c} = 0.89 \pm 0.075$, $\beta_{D_s} = 0.56 \pm 0.011$ and $\beta_{D_s^*} = 0.3376$.

Table 2. Form factors for $B_c \rightarrow D_s(1968)\ell\bar{\ell}$ decay process

	F(0)	a	b
f_+	$0.25_{-0.02}^{+0.03}$	$2.94_{-0.22}^{+0.31}$	$0.70_{-0.06}^{+0.01}$
f_-	$-0.245_{-0.10}^{+0.19}$	$3.05_{-0.27}^{+0.23}$	$0.74_{-0.02}^{+0.06}$
F_T	$-0.357_{-0.03}^{+0.04}$	$2.91_{-0.20}^{+0.19}$	$0.68_{-0.05}^{+0.07}$

Table 3. Form factors for $B_c \rightarrow D_s^*(2317)\ell\bar{\ell}$ decay process

	F(0)	a	b
u_+	$0.110_{-0.01}^{+0.02}$	$4.093_{-0.22}^{+0.67}$	$0.895_{-0.04}^{+0.01}$
u_-	$-0.144_{-0.01}^{+0.02}$	$4.235_{-0.41}^{+0.30}$	$0.988_{-0.00}^{+0.01}$
U_T	$-0.194_{-0.02}^{+0.01}$	$4.068_{-0.38}^{+0.45}$	$0.885_{-0.00}^{+0.01}$

As we have mentioned above, the physical energy region for rare leptonic decays is time-like. For $B_c \rightarrow D_s(1968)\ell\bar{\ell}$ decay process, the region is $4m_\ell^2 \leq q^2 \leq (M_{B_c} - M_{D_s})^2 = 18.56 \text{ GeV}^2$, and for $B_c \rightarrow D_s^*(2317)\ell\bar{\ell}$ decay process, the region is $4m_\ell^2 \leq q^2 \leq (M_{B_c} - M_{D_s^*})^2 = 15.67 \text{ GeV}^2$. Because the form factors in both time-like and space-like regions share the same form, we can choose the energy area in space-like region ranging from -25 GeV to 0 GeV to perform the light-cone calculation and then extract the parameters a , b and $F(0)$ in Eq. (25) with the errors coming from the uncertainties of β parameters, so we can acquire the B_c decay form factors.

With a light-cone calculation and parameters fitting, we list the parameters in the form factors f_+ , f_- , F_T , u_+ , u_- and U_T in Table 2 and Table 3.

In Figs. 1-3, we show our results of f_+ , f_- and f_T for $B_c \rightarrow D_s(1968)\ell\bar{\ell}$ decay process and compare them with other predictions [19,20,21]. As shown in the figures, the absolute magnitudes of the form factors in our results are slightly larger than those in Azizi's [19] (dotted curve), those in Geng's [20] (dashed curve) and those in Choi's [21] (dash-dotted curve) at $q^2 = 0$ point. We also compare the form factors for decay process $B_c \rightarrow D_s(1968)\ell\bar{\ell}$ with those for decay process $B_c \rightarrow D_s^*(2317)\ell\bar{\ell}$ in Figs. 4-6. We can see from the figures that the absolute magnitudes of form factors for decay process $B_c \rightarrow D_s(1968)\ell\bar{\ell}$ are about twice larger than those for $B_c \rightarrow D_s^*(2317)\ell\bar{\ell}$ process at $q^2 = 0$ point, but as q^2 become large, they tend to be the same.

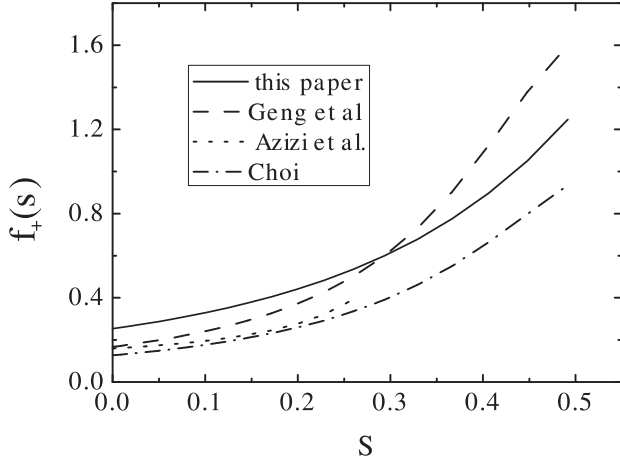


Fig. 1. $f_+(q^2)$ for $B_c \rightarrow D_s(1968)\ell\bar{\ell}$ with definition $S = q^2/M_{B_c^2}$. Our results are represented by *solid curve*, Azizi's [19] are represented by *dotted curve*, Geng's [20] are represented by *dashed curve* and Choi's [21] are represented by *dash-dotted curve* respectively.

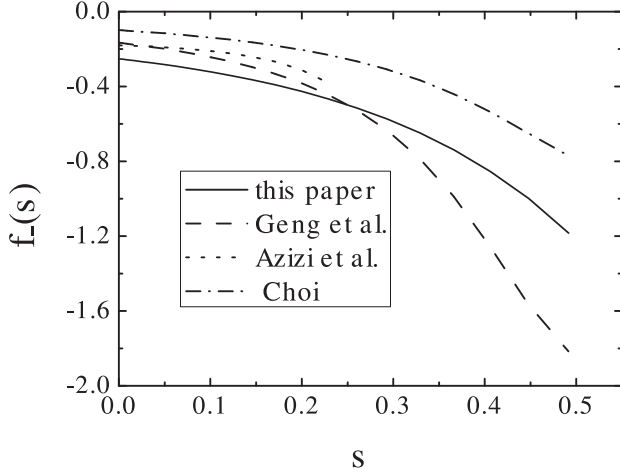


Fig. 2. $f_-(q^2)$ for $B_c \rightarrow D_s(1968)\ell\bar{\ell}$ process. Our results are represented by the *solid curve*, Azizi's [19] are represented by the *dotted curve*, Geng's [20] are represented by the *dashed curve* and Choi's [21] are represented by the *dash-dotted curve* respectively.

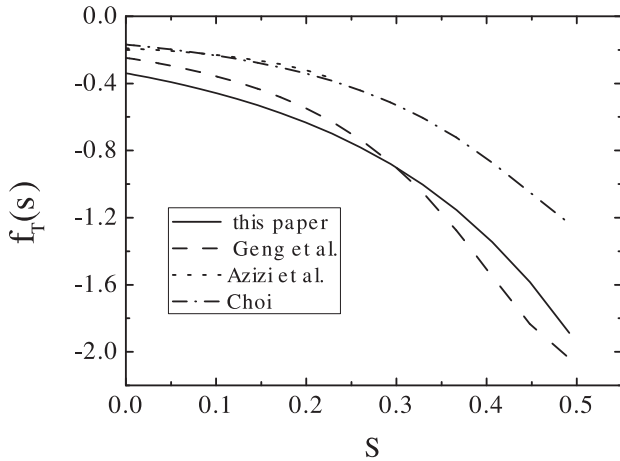


Fig. 3. $f_T(q^2)$ for $B_c \rightarrow D_s(1968)\ell\bar{\ell}$ process. Our results are represented by the *solid curve*, Azizi's [19] are represented by

the *dotted curve*, Geng's [20] are represented by the *dashed curve* and Choi's [21] are represented by the *dash-dotted curve* respectively.

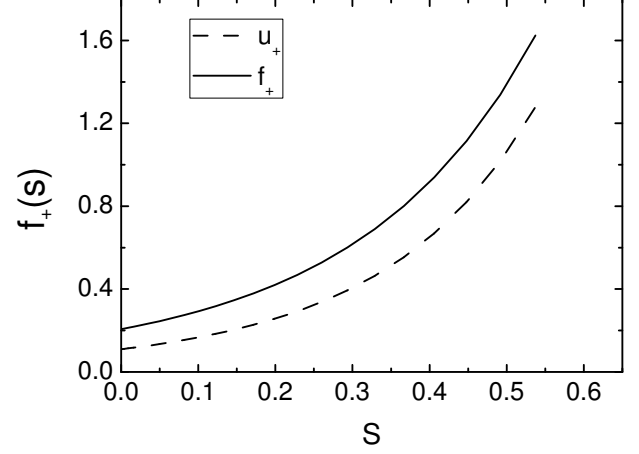


Fig. 4. $f_+(q^2)$ for $B_c \rightarrow D_s(1968)\ell\bar{\ell}$ process represented by the *solid curve* compared with $u_+(q^2)$ for $B_c \rightarrow D_s^*(2317)\ell\bar{\ell}$ process represented by the *dashed curve*.

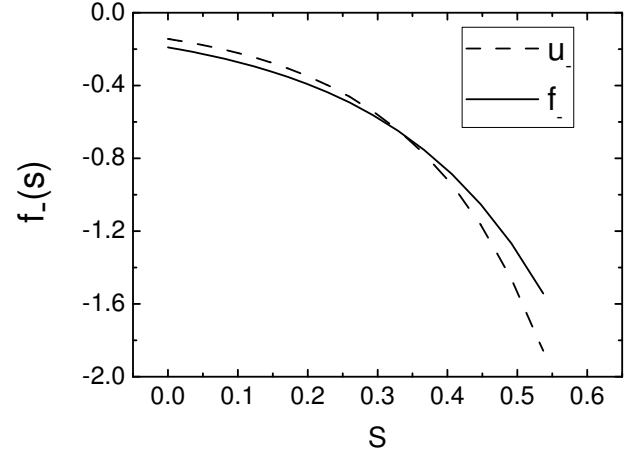


Fig. 5. $f_-(q^2)$ for $B_c \rightarrow D_s(1968)\ell\bar{\ell}$ process represented by the *solid curve* compared with $u_-(q^2)$ for $B_c \rightarrow D_s^*(2317)\ell\bar{\ell}$ process represented by the *dashed curve*.

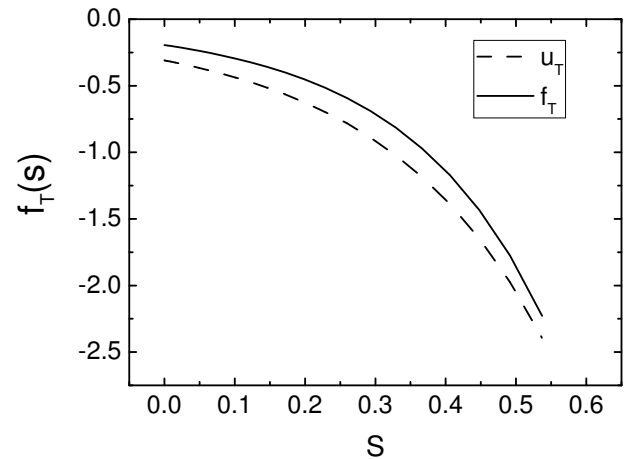


Fig. 6. $f_T(q^2)$ for $B_c \rightarrow D_s(1968)\ell\bar{\ell}$ process represented by the *solid curve* compared with $u_T(q^2)$ for $B_c \rightarrow D_s^*(2317)\ell\bar{\ell}$ process represented by the *dashed curve*.

Differential branching ratios for decay processes $B_c \rightarrow D_s^*(2317)\ell\bar{\ell}$ and $B_c \rightarrow D_s(1968)\ell\bar{\ell}$ are shown in Figs. 7-9. We only take into account the short distance effect in the effective hamiltonian, so there are no peaks at $c\bar{c}$ resonance threshold. It is interesting to notice that the form factors for the two decay processes show few differences, but the differential branching ratios of the two decay modes have large discrepancies as shown in Figs. 7-9. The maximum values of differential branching ratios for $B_c \rightarrow D_s(1968)\ell\bar{\ell}$ decay process are about 3~10 times larger than those for $B_c \rightarrow D_s^*(2317)\ell\bar{\ell}$ decay process. Longitudinal LPAs are shown in Fig. 10 and Fig. 11. It is easy to find from Fig. 10 that the LPAs for both $B_c \rightarrow D_s(1968)\mu^+\mu^-$ and $B_c \rightarrow D_s^*(2317)\mu^+\mu^-$ decay processes are close to -1 in most of the energy region, and become zero sharply at the end points of S . It can be explained by a formula [62]:

$$P_L \simeq \frac{2C_{10}\text{Re}C_9^{\text{eff}}}{|C_9^{\text{eff}}|^2 + |C_{10}^2|} \simeq -1, \quad (27)$$

when lepton mass $m_l \rightarrow 0$. However, for the case of $\ell = \tau$, because of the heavy mass of τ , the values of LPAs change remarkably with the variation of S as shown in Fig. (11).

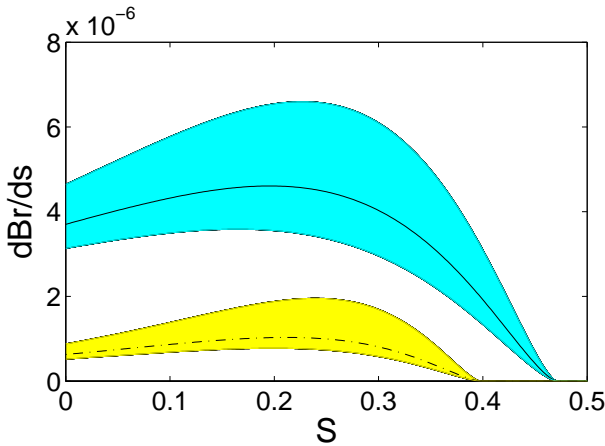


Fig. 7. Differential branching ratios of $B_c \rightarrow D_s\nu\bar{\nu}$ decay process, represented by the *solid curve*, and $B_c \rightarrow D_s^*\nu\bar{\nu}$ decay process, represented by the *dash-dotted curve*. The shaded regions show the errors.

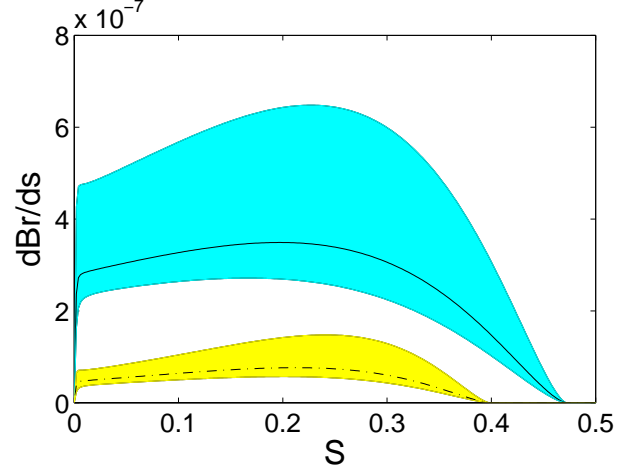


Fig. 8. Differential branching ratios of $B_c \rightarrow D_s\mu^+\mu^-$ decay process, represented by the *solid curve*, and $B_c \rightarrow D_s^*\mu^+\mu^-$ decay process, represented by the *dash-dotted curve*. The shaded regions show the errors.

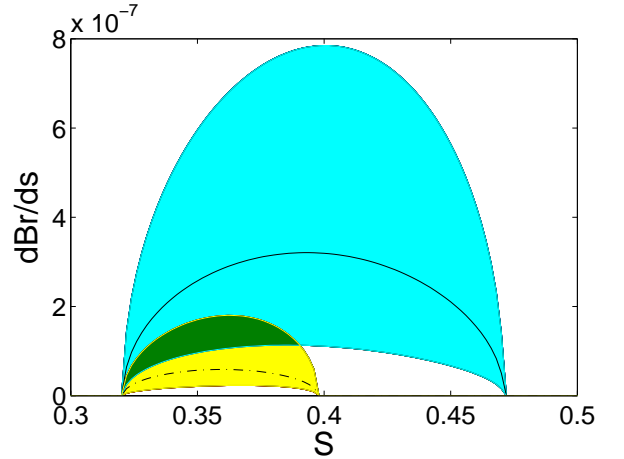


Fig. 9. Differential branching ratios of $B_c \rightarrow D_s\tau^+\tau^-$ decay process, represented by the *solid curve*, and $B_c \rightarrow D_s^*\tau^+\tau^-$ decay process, represented by the *dash-dotted curve*. The shaded regions show the errors.

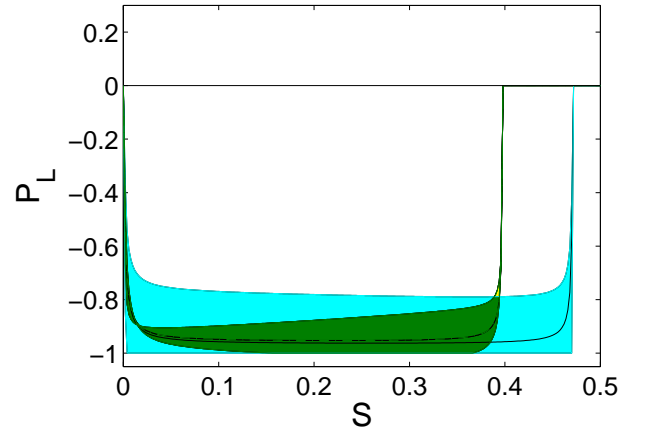


Fig. 10. Longitudinal lepton polarization asymmetries of $B_c \rightarrow D_s\mu^+\mu^-$ decay process, represented by the *solid curve*,

Table 4. Branching ratios without long distance contributions for $B_c \rightarrow D_s(1968)\ell\bar{\ell}$ decay

	our results	Azizi [19]	Geng [20]	Choi [21]
$\mathcal{B}(B_c \rightarrow D_s \nu \bar{\nu})$	$1.67^{+0.70}_{-0.39} \times 10^{-6}$	0.49×10^{-6}	0.92×10^{-6}	0.37×10^{-6}
$\mathcal{B}(B_c \rightarrow D_s \mu^+ \mu^-)$	$1.26^{+1.07}_{-0.30} \times 10^{-7}$	0.61×10^{-7}	1.36×10^{-7}	0.51×10^{-7}
$\mathcal{B}(B_c \rightarrow D_s \tau^+ \tau^-)$	$0.37^{+0.55}_{-0.24} \times 10^{-7}$	0.23×10^{-7}	0.37×10^{-7}	0.13×10^{-7}

Table 5. Branching ratios without long distance contributions for $B_c \rightarrow D_s^*(2317)\ell\bar{\ell}$ decay

	our results	SR [23]
$\mathcal{B}(B_c \rightarrow D_s^* \nu \bar{\nu})$	$3.08^{+2.46}_{-0.73} \times 10^{-7}$	$(3.06 \pm 0.76) \times 10^{-7}$
$\mathcal{B}(B_c \rightarrow D_s^* \mu^+ \mu^-)$	$2.27^{+1.92}_{-0.57} \times 10^{-8}$	$(3.76 \pm 0.92) \times 10^{-8}$
$\mathcal{B}(B_c \rightarrow D_s^* \tau^+ \tau^-)$	$3.53^{+7.30}_{-2.16} \times 10^{-9}$	$(1.28 \pm 0.32) \times 10^{-9}$

and $B_c \rightarrow D_s^* \mu^+ \mu^-$ decay process, represented by the *dash-dotted curve*. The shaded regions show the errors.

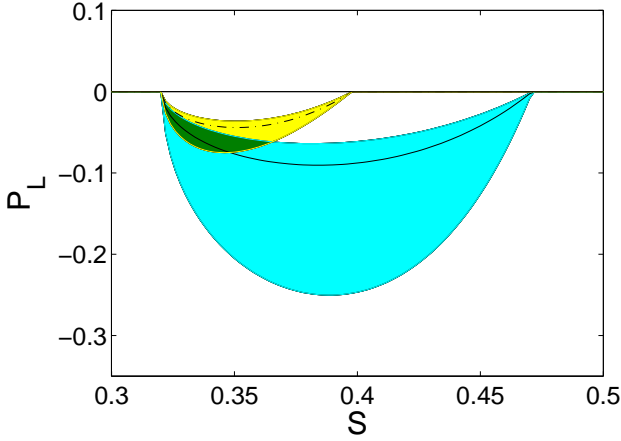


Fig. 11. Longitudinal lepton polarization asymmetries of $B_c \rightarrow D_s \tau^+ \tau^-$ decay process, represented by the *solid curve*, and $B_c \rightarrow D_s^* \tau^+ \tau^-$ decay process, represented by the *dash-dotted curve*. The shaded regions show the errors.

By integrating the differential ratios over $S = q^2/M_{B_c}^2$, we can obtain the branching ratios for the two decay processes. We list the results in Table 4 and Table 5 and compare our results with other predictions.

The average values of LPAs can also be acquired by integral. For the decay process $B_c \rightarrow D_s(1968)\ell^+\ell^-$, the average values of P_L are $-0.94^{+0.17}_{-0.06}$, $-0.07^{+0.01}_{-0.11}$ for $\ell = \mu, \tau$ respectively. For the decay process $B_c \rightarrow D_s^*(2317)\ell^+\ell^-$, the average values of P_L are $-0.93^{+0.07}_{-0.04}$, $-0.032^{+0.006}_{-0.020}$ for $\ell = \mu, \tau$ respectively.

5 Discussion and conclusion

In this work, we analyzed the rare leptonic decay processes $B_c \rightarrow D_s(1968)\ell\bar{\ell}$ and $B_c \rightarrow D_s^*(2317)\ell\bar{\ell}$ within the framework of the LCQM. We calculate the transition form factors and obtain the branching ratios of the relevant decay modes in which a ν , μ or τ lepton pair is produced at the order $10^{-6} \sim 10^{-7}$. For $B_c \rightarrow D_s(1968)\ell\bar{\ell}$ decay modes, we give a comparison of branching ratios with

other predictions. The results from our model are much larger than the results from RM and SM, and are comparable with QM. We also give our predictions of branching ratios of $B_c \rightarrow D_s^*(2317)\ell\bar{\ell}$ decay modes, and notice that they are about 80 percent smaller than the relevant ones of $B_c \rightarrow D_s(1968)\ell\bar{\ell}$ decay modes.

As the LHC started running recently, the B_c meson plays an important role in investigating the structure of hadrons and in testing the unitarity of CKM quark mixing matrix. Experiments at the LHC may not be able to measure the modes in which a neutrino pair is produced. For $B_c \rightarrow D_s(1968)\ell^+\ell^-$, candidates for $D_s(1968)$ can be reconstructed in the mode $D_s \rightarrow \phi(\rightarrow K^+K^-)\pi$ [63]. To enhance the search sensitivity, it can also be reconstructed in the modes $D_s^+ \rightarrow \bar{K}^{*0}K^+$, $D_s^+ \rightarrow K^+K_S^0$, or $D_s^+ \rightarrow \pi^+\pi^+\pi^-$ [64, 65]. If we take the mode $D_s \rightarrow \phi\pi$ of which the branching ratio is $4.5 \pm 0.4\%$ into account to reconstruct D_s , the effective branching ratio of $B_c \rightarrow D_s(\rightarrow \phi\pi)\mu^+\mu^-$ is $0.56^{+0.48}_{-0.13} \times 10^{-8}$ and that of $B_c \rightarrow D_s(\rightarrow \phi\pi)\tau^+\tau^-$ is $1.66^{+2.48}_{-1.08} \times 10^{-9}$. For $B_c \rightarrow D_s^*(2317)\ell^+\ell^-$, candidates for $D_s^*(2317)$ can be reconstructed in the mode $D_s^* \rightarrow D_s\pi^0$ [66, 67, 68]. With the branching ratios of the other decay modes of $D_s^*(2317)$ much smaller than that of $D_s\pi^0$, the search sensitivity depends mostly on the reconstruction of D_s . Therefore, the effective branching ratio of $B_c \rightarrow D_s^*(\rightarrow D_s(\rightarrow \phi\pi)\pi^0)\mu^+\mu^-$ is $1.02^{+0.86}_{-0.25} \times 10^{-9}$ and that of $B_c \rightarrow D_s^*(\rightarrow D_s(\rightarrow \phi\pi)\pi^0)\tau^+\tau^-$ is $1.59^{+3.28}_{-0.97} \times 10^{-10}$. All the results predicted in this paper can be tested in the future planned experiments at the LHC.

Acknowledgements

This work is partially supported by National Natural Science Foundation of China (Grants No. 11021092, No. 10975003, No. 11035003, and No. 11120101004).

Appendix A

The form factors $f_+(q^2)$, $F_T(q^2)$, $u_+(q^2)$, $U_T(q^2)$ can be obtained directly from the calculation of matrix elements

$\langle D_s | \bar{s} \Gamma^+ b | B_c \rangle$ in LCQM. They can be expressed in explicit forms as:

$$\begin{aligned}
f_+(q^2) &= \int_0^1 dx \int \frac{d^2 \mathbf{k}_\perp}{16\pi^3} \phi_s^*(x, \mathbf{k}'_\perp) \phi_s(x, \mathbf{k}_\perp) \\
&\quad \times \frac{\mathcal{A}_s \mathcal{A}_b + \mathbf{k}'_\perp \cdot \mathbf{k}_\perp}{\sqrt{\mathcal{A}_s^2 + \mathbf{k}'_\perp{}^2} \sqrt{\mathcal{A}_b^2 + \mathbf{k}_\perp^2}}, \\
u_+(q^2) &= \int_0^1 dx \int \frac{d^2 \mathbf{k}_\perp}{16\pi^3} \frac{\widetilde{M}_0^2}{2\sqrt{3}M_0} \phi_p^*(x, \mathbf{k}'_\perp) \phi_s(x, \mathbf{k}_\perp) \\
&\quad \times \frac{\mathcal{A}'_s \mathcal{A}_b + \mathbf{k}'_\perp \cdot \mathbf{k}_\perp}{\sqrt{\mathcal{A}_s^2 + \mathbf{k}'_\perp{}^2} \sqrt{\mathcal{A}_b^2 + \mathbf{k}_\perp^2}}, \\
F_T(q^2) &= \int_0^1 dx \int \frac{d^2 \mathbf{k}_\perp}{16\pi^3} \phi_s^*(x, \mathbf{k}'_\perp) \phi_s(x, \mathbf{k}_\perp) \\
&\quad \times \frac{x(M_{B_c} + M_{D_s}) [\mathcal{A}_b + (m_s - m_b) \frac{\mathbf{k}_\perp \cdot \mathbf{q}_\perp}{\mathbf{q}_\perp^2}]}{\sqrt{\mathcal{A}_s^2 + \mathbf{k}'_\perp{}^2} \sqrt{\mathcal{A}_b^2 + \mathbf{k}_\perp^2}}, \\
U_T(q^2) &= \int_0^1 dx \int \frac{d^2 \mathbf{k}_\perp}{16\pi^3} \frac{\widetilde{M}_0^2}{2\sqrt{3}M_0} \phi_p^*(x, \mathbf{k}'_\perp) \phi_s(x, \mathbf{k}_\perp) \\
&\quad \times \frac{x(M_{B_c} + M_{D_s^*}) [\mathcal{A}_b - (m_s + m_b) \frac{\mathbf{k}_\perp \cdot \mathbf{q}_\perp}{\mathbf{q}_\perp^2}]}{\sqrt{\mathcal{A}_s^2 + \mathbf{k}'_\perp{}^2} \sqrt{\mathcal{A}_b^2 + \mathbf{k}_\perp^2}},
\end{aligned} \tag{28}$$

where $\mathbf{k}'_\perp = \mathbf{k}_\perp - x\mathbf{q}_\perp$, $\mathcal{A}_s = m_s x + m_q(1-x)$, $\mathcal{A}_b = m_b x + m_q(1-x)$, and $\mathcal{A}_s = -m_s x + m_q(1-x)$.

For $f_-(q^2)$ and $u_-(q^2)$, we can not evaluate them by choosing the plus component of the current, so we use the \perp components of the current to obtain $f_-(q^2)$ and $u_-(q^2)$:

$$\begin{aligned}
\langle D_s | \bar{s}(\mathbf{q}_\perp \cdot \gamma_\perp) \gamma_5 b | B_c \rangle &= \mathbf{q}_\perp^2 [f_+(q^2) - f_-(q^2)] \\
&= \int \frac{dx d^2 \mathbf{k}_\perp}{16\pi^3} \frac{x \phi_s^*(x, \mathbf{k}'_\perp) \phi_s(x, \mathbf{k}_\perp)}{\sqrt{\mathcal{A}_s^2 + \mathbf{k}'_\perp{}^2} \sqrt{\mathcal{A}_b^2 + \mathbf{k}_\perp^2}} \\
&\quad \times \left\{ \frac{\mathcal{A}_b^2 + \mathbf{k}_\perp^2}{(1-x)x} (\mathbf{k}_\perp + \mathbf{q}_\perp) \cdot \mathbf{q}_\perp - \frac{\mathcal{A}_s^2 + \mathbf{k}'_\perp{}^2}{(1-x)x} \mathbf{k}_\perp \cdot \mathbf{q}_\perp \right. \\
&\quad \left. + [(-m_s + m_b)^2 + \mathbf{q}_\perp^2] \mathbf{k}_\perp \cdot \mathbf{q}_\perp \right\},
\end{aligned} \tag{29}$$

$$\begin{aligned}
\langle D_s^* | \bar{s}(\mathbf{q}_\perp \cdot \gamma_\perp) \gamma_5 b | B_c \rangle &= \mathbf{q}_\perp^2 [u_+(q^2) - u_-(q^2)] \\
&= \int \frac{dx d^2 \mathbf{k}_\perp}{16\pi^3} \frac{\widetilde{M}_0^2}{2\sqrt{3}M_0} \frac{x \phi_p^*(x, \mathbf{k}'_\perp) \phi_s(x, \mathbf{k}_\perp)}{\sqrt{\mathcal{A}_s^2 + \mathbf{k}'_\perp{}^2} \sqrt{\mathcal{A}_b^2 + \mathbf{k}_\perp^2}} \\
&\quad \times \left\{ \frac{\mathcal{A}_b^2 + \mathbf{k}_\perp^2}{(1-x)x} (\mathbf{k}_\perp + \mathbf{q}_\perp) \cdot \mathbf{q}_\perp - \frac{\mathcal{A}'_s{}^2 + \mathbf{k}'_\perp{}^2}{(1-x)x} \mathbf{k}_\perp \cdot \mathbf{q}_\perp \right. \\
&\quad \left. + [(m_s + m_b)^2 + \mathbf{q}_\perp^2] \mathbf{k}_\perp \cdot \mathbf{q}_\perp \right\}.
\end{aligned} \tag{30}$$

References

1. T. Huang, X.G. Wu, M.Z. Zhou, Phys. Lett. B **611**, 260 (2005).
2. J.P. Ma, Q. Wang, Phys. Lett. B **613**, 39 (2005).
3. H.N. Li, H.S. Liao, Phys. Rev. D **70**, 074030 (2004).
4. X.G. He, Y.K. Hsiao, J.Q. Shi, Y.L. Wu, Y.F. Zhou, Phys. Rev. D **64**, 034002 (2001).
5. X.G. He, C.S. Li, L.L. Yang, Phys. Rev. D **71**, 054006 (2005).
6. D.S. Du, C. Liu, D.X. Zhang, Phys. Lett. B **317**, 179 (1993).
7. Y. Li, C.D. Lu, Z.J. Xiao, X.Q. Yu, Phys. Rev. D **70**, 034009 (2004).
8. Y.L. Wu, Y.F. Zhou, Phys. Rev. D **71**, 021701(R) (2005).
9. D.S. Du, H.Y. Jin, Y.D. Yang, Phys. Lett. B **414**, 130 (1997).
10. Z.J. Xiao, K.T. Chao, C.S. Li, Phys. Rev. D **65**, 114021 (2002).
11. C.H. Chang, Y.Q. Chen, Phys. Rev. D **46**, 3845 (1992).
12. C.H. Chang, Y.Q. Chen, Phys. Rev. D **48**, 4086 (1993).
13. C.H. Chang, Y.Q. Chen, Phys. Lett. B **284**, 127 (1992).
14. C.H. Chang, C. Driouichi, P. Eerola, X.G. Wu, Comput. Phys. Commun. **159**, 192 (2004).
15. C.H. Chang, X.G. Wu, Eur. Phys. J. C **38**, 267 (2004).
16. C.H. Chang, C.F. Qiao, J.X. Wang, X.G. Wu, Phys. Rev. D **71**, 074012 (2005).
17. C.H. Chang, J.X. Wang, X.G. Wu, Phys. Rev. D **77**, 014022 (2008).
18. M.S. Alam et al. (CLEO Collaboration), Phys. Rev. Lett. **74**, 2885 (1995).
19. K. Azizi, R. Khosravi, Phys. Rev. D **78**, 036005 (2008).
20. C.Q. Geng, C.W. Hwang, C.C. Liu, Phys. Rev. D **65**, 094037 (2002).
21. H.M. Choi, Phys. Rev. D **81**, 054003 (2010).
22. A. Faessler, T. Gutsche, M.A. Ivanov, J.G. Korner, V.E. Lyubovitskij, Eur. Phys. J. C **4**, 18 (2002).
23. N. Ghahramany, R. Khosravi, Z. Naseri Phys. Rev. D **81**, 036005 (2010).
24. B. Aubert et al. (BaBar Collaboration), Phys. Rev. Lett. **90**, 242001 (2003).
25. S. Godfrey, N. Isgur, Phys. Rev. D **32**, 189 (1985).
26. S. Godfrey, R. Kokoski, Phys. Rev. D **43**, 1679 (1991).
27. T. Barnes, F.E. Close, H.J. Lipkin, Phys. Rev. D **68**, 054006 (2003).
28. A.P. Szczepaniak, Phys. Lett. B **567**, 23 (2003).
29. H.Y. Cheng, W.S. Hou, Phys. Lett. B **566**, 193 (2003).
30. W.A. Bardeen, E.J. Eichten, C.T. Hill, Phys. Rev. D **68**, 054024 (2003).
31. M.A. Nowak, M. Rho, I. Zahed, Acta. Phys. Pol. B **35**, 2377 (2004).
32. G.P. Lepage, S.J. Brodsky, Phys. Rev. D **22**, 2157 (1980).
33. S.J. Brodsky, T. Huang, G.P. Lepage, in *Particles and Fields-2*, Proceedings of the Banff Summer Institute, Banff, Alberta, 1981, edited by A.Z. Capri and A.N. Kamal (Plenum, New York, 1983), p. 143.
34. S.J. Brodsky, H.C. Pauli, S.S. Pinsky, Phys. Rep. **301**, 299 (1998).
35. H.Y. Cheng, C.Y. Cheung, C.W. Hwang, Phys. Rev. D **55**, 1559 (1997).
36. H.Y. Cheng, C.K. Chua, C.W. Hwang, Phys. Rev. D **69**, 074025 (2004).
37. H.M. Choi, C.R. Ji, L.S. Kisslinger, Phys. Rev. D **65**, 074032 (2002).
38. J.H. Yu, T. Wang, C.R. Ji, B.-Q. Ma, Phys. Rev. D **76**, 074009 (2007).

39. T. Huang, B.-Q. Ma, Q.-X. Shen, Phys. Rev. D **49**, 1490 (1994).
40. B.-Q. Ma, T. Huang, J. Phys. G **21**, 765 (1995).
41. B. Grinstein, M.B. Wise, M.J. Savage Nucl. Phys. B **319**, 271 (1989).
42. A.J. Buras, M. Münz, Phys. Rev. D **52**, 186 (1995).
43. C.S. Lim, T. Morozumi, A.I. Sanda, Phys. Lett. B **218**, 343 (1989).
44. N.G. Deshpande, J. Trampetic, K. Panose, Phys. Rev. D **39**, 1461 (1989).
45. M. Wirbel, S. Stech, M. Bauer, Z. Phys. C **29**, 637 (1985).
46. C.Q. Geng, C.P. Kao, Phys. Rev. D **54**, 5636 (1996).
47. B.-Q. Ma, Z. Phys. A **345**, 321 (1993).
48. B.-W. Xiao, X. Qian, B.-Q. Ma, Eur. Phys. J. A **15**, 523 (2002).
49. B.-W. Xiao, B.-Q. Ma, Phys. Rev. D **68**, 034020 (2003).
50. B.-W. Xiao, B.-Q. Ma, Phys. Rev. D **71**, 014034 (2005).
51. E. Wigner, Ann. Math. **40**, 149 (1939).
52. H.J. Melosh, Phys. Rev. D **9**, 1095 (1974).
53. B.-Q. Ma, J. Phys. G **17**, L53 (1991) [arXiv:0711.2335 [hep-ph]]
54. B.-Q. Ma and Q.-R. Zhang, Z. Phys. C **58**, 479 (1993)
55. S.D. Drell, T.M. Yan, Phys. Rev. Lett. **24**, 181 (1970).
56. G. West, Phys. Rev. Lett. **24**, 1206 (1970).
57. C.R. Ji, H.M. Choi, Phys. Lett. B **513**, 330 (2001).
58. C.Amsler et al. (Particle Data Group), Phys. Lett. B **667**, 1 (2008).
59. X.X. Wang, W. Wang, C.D. Lu, Phys. Rev. D **79**, 114018 (2009).
60. A.S. Kronfeld, arXiv:0912.0543 [hep-ph]
61. H.Y. Cheng, C.K. Chua, C.W. Hwang, Phys. Rev. D **69**, 074025 (2004).
62. G. Burdman, Phys. Rev. D **52**, 6400 (1995).
63. T. Aaltonen et al. (CDF Collaboration), Phys. Rev. Lett. **103**, 191802 (2009).
64. T. Aaltonen et al. (CDF Collaboration), Phys. Rev. Lett. **100**, 021803 (2008).
65. R. Louvot et al. (Belle Collaboration), Phys. Rev. Lett. **102**, 021801 (2009).
66. D. Besson et al. (CLEO Collaboration), Phys. Rev. D **68**, 032002 (2003).
67. B. Aubert et al. (BaBar Collaboration), Phys. Rev. D **69**, 031101 (2004).
68. B. Aubert et al. (BaBar Collaboration), Phys. Rev. Lett. **93**, 181801 (2004).